

Antiproton Production in 11.5A GeV/c Au + Pb Nucleus-Nucleus Collisions

T. A. Armstrong,⁷ K. N. Barish,^{11,*} M. J. Bennett,^{11,†} S. J. Bennett,¹⁰ A. Chikanian,¹¹ S. D. Coe,¹¹ T. M. Cormier,¹⁰ R. Davies,⁸ G. De Cataldo,¹ P. Dee,^{10,‡} G. E. Diebold,¹¹ C. B. Dover,^{2,§} P. Fachini,¹⁰ L. E. Finch,¹¹ N. K. George,¹¹ N. Giglietto,¹ S. V. Greene,⁹ P. Haridas,⁶ J. C. Hill,⁴ A. S. Hirsch,⁸ H. Z. Huang,^{3,||} B. Kim,¹⁰ B. S. Kumar,^{11,¶} J. G. Lajoie,¹¹ R. A. Lewis,⁷ Q. Li,¹⁰ Y. Li,¹⁰ B. Libby,^{4,**} R. D. Majka,¹¹ M. G. Munhoz,¹⁰ J. L. Nagle,^{11,††} I. A. Pless,⁶ J. K. Pope,¹¹ N. T. Porile,⁸ C. A. Pruneau,¹⁰ M. S. Z. Rabin,⁵ A. Raino,¹ J. D. Reid,^{7,‡‡} A. Rimai,^{8,§§} F. S. Rotondo,¹¹ J. Sandweiss,¹¹ R. P. Scharenberg,⁸ A. J. Slaughter,¹¹ G. A. Smith,⁷ P. Spinelli,¹ B. K. Srivastava,⁸ M. L. Tincknell,⁸ W. S. Toothacker,⁷ G. Van Buren,⁶ W. K. Wilson,¹⁰ F. K. Wohn,⁴ E. J. Wolin,^{11,|||} and K. Zhao¹⁰

(The E864 Collaboration)

¹University of Bari/INFN, Bari, Italy

²Brookhaven National Laboratory, Upton, New York 11973

³University of California at Los Angeles, Los Angeles, California 90024

⁴Iowa State University, Ames, Iowa 50011

⁵University of Massachusetts, Amherst, Massachusetts 01003

⁶Massachusetts Institute of Technology, Cambridge, Massachusetts 02139

⁷Pennsylvania State University, University Park, Pennsylvania 16802

⁸Purdue University, West Lafayette, Indiana 47907

⁹Vanderbilt University, Nashville, Tennessee 37235

¹⁰Wayne State University, Detroit, Michigan 48201

¹¹Yale University, New Haven, Connecticut 06520

(Received 13 February 1997)

We present the first results from the E864 Collaboration on the production of antiprotons in 10% central 11.5A GeV/c Au + Pb nucleus collisions at the Brookhaven Alternating Gradient Synchrotron. We report invariant multiplicities for antiproton production in the kinematic region $1.4 < y < 2.2$ and $50 < p_T < 300$ MeV/c, and compare our data with a first collision scaling model and previously published results from the E878 Collaboration. The differences between the E864 and E878 antiproton measurements and the implications for antihyperon production are discussed. [S0031-9007(97)04466-9]

PACS numbers: 25.75.Dw

The yield of antiprotons (\bar{p}) in high energy heavy-ion collisions is of considerable interest for several reasons. Models of heavy-ion collisions that include a quark-gluon plasma (QGP) phase predict that the production of antimatter will be enhanced in these collisions due to the lower quark-antiquark production threshold relative to that of a baryon-antibaryon pair [1]. Enhanced production of antimatter may also indicate strong, density dependent mean field effects [2]. The observed yield is, however, a result of both production and subsequent annihilation. Detailed study of \bar{p} production has been proposed as an indirect way of measuring the baryon density in these collisions [3]. Finally, \bar{p} measurements at the Brookhaven Alternating Gradient Synchrotron (AGS) may contain a large feed-down contribution from the decay of the antilambda, $\bar{\Lambda} \rightarrow \bar{p} + \pi^+$, as well as other antihyperons (\bar{Y}). By comparing results from experiments with different sensitivities to \bar{p} 's from these decays, we may be able to infer the relative production of antihyperons and \bar{p} 's in Au + Pb collisions.

Experiment 864 is a high rate, large acceptance spectrometer designed to search for novel forms of matter created in heavy-ion collisions. The spectrometer consists of two dipole bending magnets (M1 and M2), with time-of-flight (TOF) hodoscopes and straw tube tracking cham-

bers downstream of the second magnet (see Fig. 1). The scintillation counter hodoscopes (H1, H2, and H3) provide space points for tracking, as well as redundant charge and TOF measurements. The TOF resolution is ~ 130 ps in each plane. The straw tube chambers (S2 and S3) provide high precision space points. The mass resolution of the spectrometer is between 3% and 5% in the kinematic region explored in this data set. At the end of the apparatus is a lead/scintillating fiber hadronic calorimeter, which

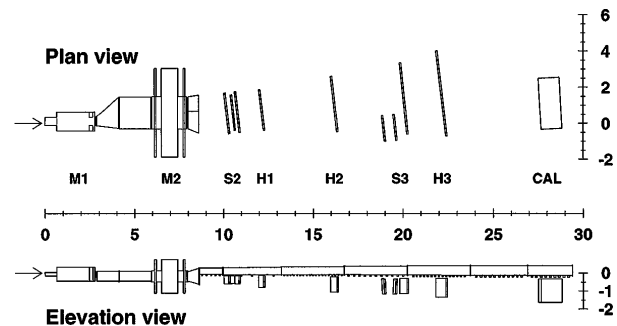


FIG. 1. The E864 spectrometer (1994 configuration). Note that the calorimeter and S3 U, V layers are incomplete. The Au beam is incident on a Pb target from the left, and the scale shown is in meters. The vacuum chamber downstream of M2 is not shown in the plan view. See text for details.

is used to confirm the energy of the particle determined by the tracking detectors [4]. Finally, a straw tube chamber (S1) located between the spectrometer magnets provides additional background rejection. The uninteracted beam is contained above the experiment in a large vacuum chamber. The centrality (impact parameter) of the collision is determined by a segmented scintillation counter located near the target, which measures charged particle multiplicity in the polar angular range of 16.6° to 45° with respect to the incident beam. For this analysis we selected events with the 10% largest pulse heights in the multiplicity array, roughly corresponding to the 10% most central events or an impact parameter $b \leq 4.7$ fm. A complete description of the apparatus is in preparation [5].

The data presented in this paper are derived from 20.1×10^6 10% central Au + Pb interactions collected during the 1994 run with 5%, 10%, and 20% Pb targets. For the 1994 run, the experimental apparatus was not complete. The calorimeter was $\frac{1}{4}$ complete, two layers of the S3 straw array were only $\frac{1}{3}$ complete, and S1 was not in place. The calorimeter was stacked to have optimal acceptance for neutral particles, and thus was not used in this analysis. An average of five tracks per event was found in the spectrometer. The mass of a particle is calculated as $m = Z \frac{r}{\beta\gamma}$ where the rigidity r is reconstructed from the downstream fit of the track in the bend plane, and the charge Z and velocity β are measured by the hodoscopes. Antiproton candidates are selected by a set of quality cuts on the fits to the particle track in the detector. Additional cuts are made to exclude particles whose back projection intercepts the collimator in the first spectrometer magnet and to demand a charge measurement consistent with $Z = 1$ in each hodoscope. The resulting mass distribution is fit to a combination of a Gaussian signal and linear background in the mass region of the \bar{p} . The ratio of the number of signal counts in $\pm 3\sigma$ about the fixed \bar{p} peak to the number of background counts is ~ 3 . The measured \bar{p} yields are corrected for the experimental acceptance and efficiencies in each rapidity and p_T bin. Since the TOF information from all three hodoscopes is required for a track in the spectrometer, an occupancy dependent correction is made to account for the fact that if a faster track hits a hodoscope slat first, later tracks could be lost, because only the first time will be recorded.

The \bar{p} invariant multiplicities measured in E864 are shown in Fig. 2. The measured multiplicities are approximately flat over the p_T range where the experiment has acceptance, and correspond to a level of $1.5 \times 10^{-2} \text{ GeV}^{-2} c^2$ at midrapidity ($y = 1.6$). Invariant multiplicities for \bar{p} production as measured by the E878 Collaboration [6] are also shown in Fig. 2. The E878 data have been scaled up by a factor of 1.5 to account for the lower beam momentum of 10.8A GeV/c using the procedure in [7]. We estimate that there is a 15% systematic uncertainty in this energy scaling based on a comparison with fits to higher energy pp data [8]. It should also be noted that the E878 measurements are for Au + Au nu-

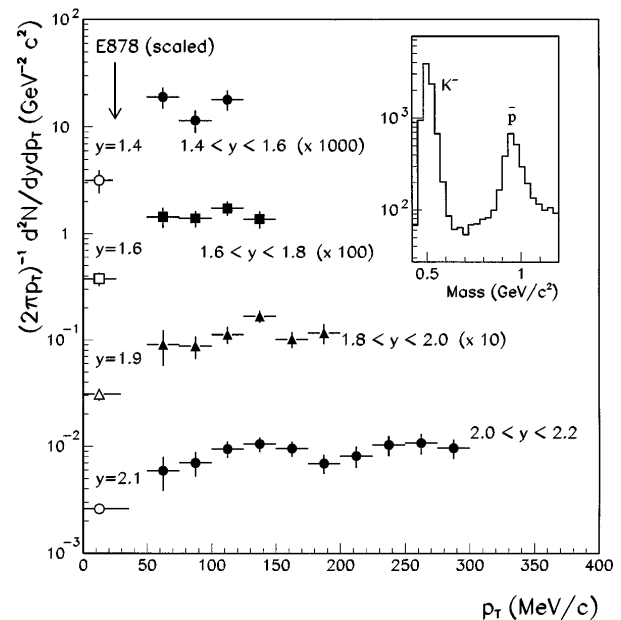


FIG. 2. \bar{p} invariant multiplicities as measured in E864 and E878, for 10% central Au + Pb and Au + Au collisions. The E878 data have been scaled up by a factor of 1.5 to account for the lower beam momentum of 10.8A GeV/c. The errors bars are statistical only. The inset shows the mass distribution measured in E864 in the \bar{p} mass region. Note the logarithmic scale.

cleus collisions; however, the difference between the Au ($Z = 79, A = 197$) and Pb ($Z = 82, A = 208$) target nuclei is negligible. We estimate the systematic errors in our measurements to be 20%, dominated by our understanding of the experimental acceptance and track quality cut efficiencies. E878 reports a systematic error of 30% on their measurements [6]. Figure 2 shows that the E864 measurements are consistently higher than their E878 counterparts.

Since the E864 data are approximately flat as a function of p_T in each rapidity interval, they are averaged in each rapidity range and extrapolated to $p_T = 0$. If we assume a Boltzmann shape to the \bar{p} distribution with a temperature parameter of 200 MeV (similar to preliminary measurements for \bar{p} 's by the E866 Collaboration [9]), this extrapolation could underestimate the invariant multiplicity at $p_T = 0$ by 6%. It should be noted that we cannot rule out a drastic change in \bar{p} production between $0 < p_T < 50$ MeV/c. If there is such a low- p_T dependence to \bar{p} production, this extrapolation will not be valid. Figure 3 shows the E864 extrapolations to $p_T = 0$ along with the scaled E878 measurements. The E878 measurements yield a rapidity width of $\sigma_y = 0.62 \pm 0.03$ [6], while the E864 data yield a width of 0.49 ± 0.05 . Using the E864 measurement extrapolated to $p_T = 0$, we can quantify the difference between E864 and E878. At midrapidity the ratio of invariant multiplicities is $3.96 \pm 0.42(\text{stat})^{+5.98}_{-1.77}(\text{syst})$. This ratio decreases as one moves away from central rapidity. We will proceed by comparing the measured \bar{p} production in

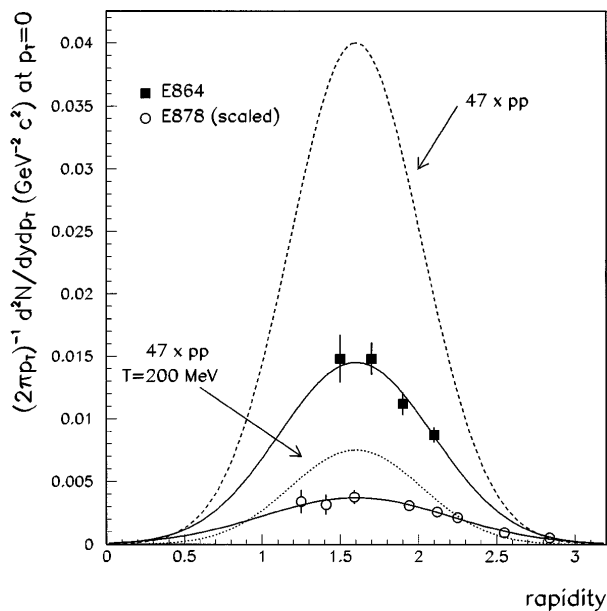


FIG. 3. \bar{p} invariant multiplicities as extrapolated to $p_T = 0$ in E864 and measured in E878 (scaled to 11.5A GeV/c), for 10% central Au + Pb and Au + Au collisions. Fits to the E864 and E878 data are also shown. The errors are statistical only. Two predictions based on first collision scaling (without annihilation) are also indicated.

E864 with a simple model, and then return to the discrepancy between the E864 and E878 measurements and its implications for antihyperon production.

If we assume a model in which \bar{p} 's are produced only in first collisions between target and projectile nucleons, and are not annihilated, we can estimate the \bar{p} yield by scaling \bar{p} production in nucleon-nucleon collisions by the number of first collisions in a nucleus-nucleus interaction. A first collisions model of this type provides a reference level of production for comparison, and may provide an indication as to whether \bar{p} production is substantially enhanced in nucleus-nucleus collisions, or suppressed (by annihilation). It has been estimated that there are typically 47 first collisions between nucleons in 10% central Au + Au(Pb) collisions [10]. We estimate the \bar{p} production in pp collisions using RQMD (v2.2) [11], which is tuned to measured \bar{p} production at higher energies and includes energy scaling of the cross section. The result of multiplying the RQMD pp invariant \bar{p} yield at $p_T = 0$ by the expected number of first collisions in a Au + Pb collision is shown in Fig. 3. In pp collisions \bar{p} production is peaked at low p_T , and the RQMD distribution can be described by a Boltzmann temperature of ~ 80 MeV. In nucleus-nucleus collisions, rescattering and annihilation are expected to broaden the distribution in rapidity and p_T . In Fig. 3 we also show the invariant yield at $p_T = 0$ assuming the same integrated yield (47 times the RQMD pp level) and a Boltzmann temperature of 200 MeV. In this case, the yield at $p_T = 0$ is somewhat lower than the yield measured in E864. This could be an indication of enhanced \bar{p} production in Au + Pb nu-

cleus collisions that more than offsets any losses due to annihilation.

In general, the \bar{p} 's detected could also be the decay products of antihyperons, such as the $\bar{\Lambda}$, $\bar{\Sigma}^0$, and the $\bar{\Sigma}^+$. The decay of the $\bar{\Sigma}^0$ will produce additional $\bar{\Lambda}$'s which will be indistinguishable from those created in the primary collision. The decay of the $\bar{\Lambda}$ and the $\bar{\Sigma}^+$ will produce \bar{p} 's whose production vertices do not coincide with the location of the primary interaction between the two nuclei. Therefore, the degree to which \bar{p} 's from these decays contribute to a measurement of \bar{p} production will vary among experiments.

Because of its large acceptance, the E864 spectrometer will detect \bar{p} 's from \bar{Y} decay. E864 does not have sufficient vertical resolution to reject \bar{p} 's from \bar{Y} decay based on the vertical projection of a particle to the target, and the analysis cuts do not preferentially reject antiprotons from \bar{Y} decay. Therefore, the \bar{p} 's detected in E864 are a combination of primary \bar{p} 's and \bar{p} 's from \bar{Y} decay, in a ratio that reflects their production ratio. The E878 Collaboration have also evaluated the acceptance of their spectrometer for feed down from \bar{Y} decay [12]. At midrapidity the acceptance for \bar{p} 's from $\bar{\Lambda}$ and $\bar{\Sigma}^0$ decay is 14% of the spectrometer acceptance for primordial \bar{p} 's, and 10% of the \bar{p} acceptance for $\bar{\Sigma}^+$ decays.

Since both E878 and E864 measure a different combination of primordial \bar{p} production and feed down from \bar{Y} decay, we can in principle separate the two components if we make two explicit assumptions: both E864 and E878 understand their systematic errors, and the entire difference between the two experiments can be attributed to antihyperon feed down. It is important to note that in energy scaling the E878 results we have implicitly assumed that the \bar{Y} 's scale with energy by the same factor as the \bar{p} 's. A detailed statistical analysis of the \bar{Y}/\bar{p} ratio as a function of the E864 and E878 measurements (see Fig. 4 for details), and the relevant statistical and systematic errors involved, shows that

$$\left(\frac{\bar{Y}}{\bar{p}}\right)_{y=1.6, p_T=0} \approx \left(\frac{\bar{\Lambda} + \bar{\Sigma}^0 + 1.1\bar{\Sigma}^+}{\bar{p}}\right) > 2.8 \text{ (98\% C.L.)}, \quad (1)$$

while the most probable value of this ratio is ~ 5 . The factor of 1.1 multiplying the $\bar{\Sigma}^+$ arises due to the different branching ratio and acceptance for the $\bar{\Sigma}^+$ compared to the $\bar{\Lambda}$. This indicates an \bar{Y}/\bar{p} ratio in Au + Pb collisions that is significantly greater than one at midrapidity and $p_T = 0$. It should be noted that if the \bar{Y} 's and the \bar{p} are produced with different distributions in y and p_T , then the ratio of integrated yields of these particles will differ from the ratio at central rapidity and $p_T = 0$. Preliminary results from Si + Au collisions based on direct measurements of \bar{p} and $\bar{\Lambda}$ production by the E859 Collaboration also indicate a ratio of integrated yields greater than one [13]. In contrast, the ratio in pp collisions at similar energies is ~ 0.2 [14].

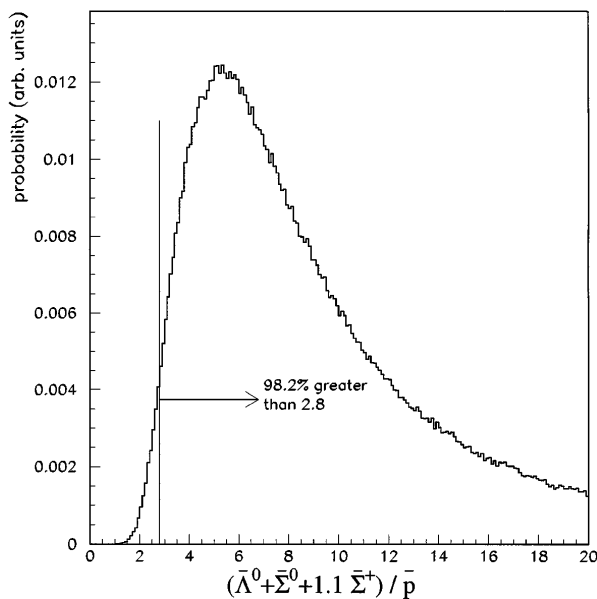


FIG. 4. The probability distribution for the ratio $(\bar{\Lambda} + \bar{\Sigma}^0 + 1.1\bar{\Sigma}^+)/\bar{p}$ at midrapidity and $p_T = 0$ extracted from the E878 and E864 measurements. This distribution is generated by varying the E878 and E864 measurements within their systematic and statistical errors. Statistical errors are treated as Gaussian, while systematic errors are treated as indicating a flat range within which the measurements may vary.

An enhancement of antihyperons arises naturally in models that include a QGP, and therefore enhanced anti-matter and strangeness production [1]. Thermal models that use a temperature and baryon chemical potential derived from measured particle spectra also indicate that the primordial $\bar{\Lambda}/\bar{p}$ ratio could be larger than one [15]. However, these models are typically used to compare integrated yields while we have only inferred the \bar{Y}/\bar{p} ratio at a point in phase space.

In comparing the results of two experiments the potential exists for differences in the overall normalization. We note that preliminary measurements of protons, K^- , deuterons, and He^3 in E864 are consistent with preliminary E878 measurements within the quoted statistical and systematic errors of both experiments [16].

In summary, E864 has measured \bar{p} production about midrapidity in Au + Pb collisions at 11.5A GeV/c. The measured \bar{p} yields at midrapidity and $p_T = 0$ are larger than those measured by the E878 Collaboration by a factor $3.96 \pm 0.42(\text{stat})^{+5.08}_{-1.77}(\text{syst})$. If we interpret the difference between E864 and E878 as a measure of \bar{Y} production, we can infer that \bar{Y}/\bar{p} is much greater than one at midrapidity and $p_T = 0$.

We would like to acknowledge the efforts of the AGS and Tandem staff in providing the beam. This work was supported by grants from the Department of Energy (DOE) High Energy Physics Division, DOE Nuclear Division, and the National Science Foundation. We would like to thank Heinz Sorge for his assistance with the RQMD calculations and Sid Kahana for illuminating discussions.

*Present address: University of California at Los Angeles, Los Angeles, CA 90024.

†Present address: University of California Space Sciences Laboratory, Berkeley, CA 94720.

‡Present address: Positron Imaging Centre, Birmingham University, Birmingham, England.

§Deceased.

||Formerly at Purdue University.

¶Present address: McKinsey & Co., New York, NY 10022.

**Present address: Department of Radiation Oncology, Medical College of Virginia, Richmond, VA 23298.

††Present address: Columbia University, Nevis Laboratory, Irvington, NY 10533.

‡‡Present address: Vanderbilt University, Nashville, TN 37235.

§§Present address: Institut de Physique Nucléaire, 91406 Orsay Cedex, France.

|||Present address: College of William and Mary, Williamsburg, VA 23185.

- [1] P. Koch, B. Müller, H. Stöcker, and W. Greiner, *Mod. Phys. Lett. A* **8**, 737 (1988); J. Ellis, U. Heinz, and Henry Kowalski, *Phys. Lett. B* **233**, 223 (1989); U. Heinz, P.R. Subramanian, H. Stöcker, and W. Greiner, *J. Phys. G* **12**, 1237 (1986).
- [2] V. Koch, G.E. Brown, and C.M. Ko, *Phys. Lett. B* **265**, 29 (1991); J. Schaffner, I.N. Mishustin, L.M. Satarov, H. Stöcker, and W. Greiner, *Z. Phys. A* **341**, 47 (1991).
- [3] P. Koch and C.B. Dover, *Phys. Rev. C* **40**, 145 (1989); S. Gavin, M. Gyulassy, M. Plümer, and R. Venugopalan, *Phys. Lett. B* **234**, 175 (1990).
- [4] The E864 Collaboration, C. A. Pruneau *et al.*, in *Proceedings of the VI International Conference on Calorimetry in High Energy Physics, Frascati, Italy, 1996*, edited by A. Antonelli, S. Bianco, A. Calcaterra, and F.L. Fabbrì (Laboratori Nazionali di Frascati dell'INFN, Frascati, 1996).
- [5] T. Armstrong *et al.* (to be published).
- [6] D. Beavis *et al.*, *Phys. Rev. Lett.* **75**, 3633 (1995).
- [7] S.H. Kahana, Y. Pang, T. Schlagel, and C.B. Dover, *Phys. Rev. C* **47**, 1356 (1993).
- [8] J. Costales, Ph.D. thesis, Massachusetts Institute of Technology, 1990.
- [9] The E866 Collaboration, H. Sako *et al.*, in *Heavy Ion Physics at the AGS (HIPAGS 96)*, edited by C. A. Pruneau, G. Welke, R. Bellweid, S.J. Bennett, J.R. Hall, and W.K. Wilson (Wayne State University Report No. WSU-NP-96-16, 1996).
- [10] B.S. Kumar, S.V. Greene, and J.T. Mitchell, *Phys. Rev. C* **50**, 2152 (1994).
- [11] H. Sorge, *Phys. Rev. C* **52**, 3291 (1995); M. Gonin *et al.*, *Phys. Rev. C* **51**, 310 (1995).
- [12] M. Bennett *et al.*, *Phys. Rev. C* **56**, 1521 (1997).
- [13] The E859 Collaboration, Y. Wu *et al.*, in *HIPAGS 96* (Ref. [9]).
- [14] V. Blobel *et al.*, *Nucl. Phys.* **B69**, 454 (1974); A.M. Rossi *et al.*, *Nucl. Phys.* **B84**, 269 (1975).
- [15] P. Braun-Munzinger, J. Stachel, J.P. Wessels, and N. Xu, *Phys. Lett. B* **344**, 43 (1995).
- [16] K. Pope, Ph.D. thesis Yale University, 1997; The E864 Collaboration, J. Lajoie *et al.*, in *HIPAGS 96* (Ref. [9]).